Inorganic Chemistry

Open Access
This article is licensed under CC-BY 4.0

pubs.acs.org/IC
Article

Stereochemically Active Lone Electron Pairs in the Chalcogen Oxide-Carbonates $Te[CO_3]O$ and $Te_4O_7[CO_3]$ at Elevated Pressures

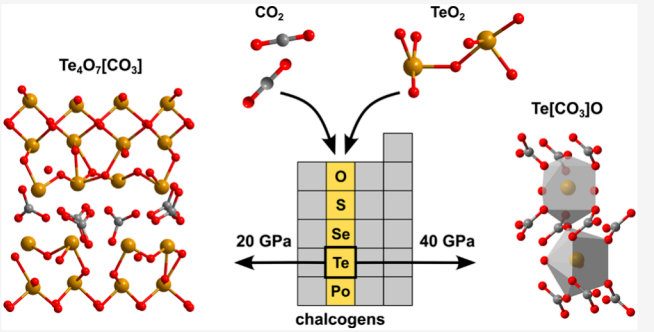
Dominik Spahr,* Lkhamsuren Bayarjargal, Ninel Sharapova, Valentin Kovalev, Andrey Aslandukov, Fariia I. Akbar, Elena Bykova, Maxim Bykov, Victor Milman, Nico Giordano, and Björn Winkler

Cite This: Inorg. Chem. 2026, 65, 17749−17755

Read Online

ACCESS | Metrics & More | Article Recommendations | Supporting Information

ABSTRACT: Two anhydrous tellurium carbonates, $Te[CO_3]O$ and $Te_4O_7[CO_3]$, have been synthesized in laser-heated diamond anvil cells by a reaction of TeO_2 with CO_2. $Te[CO_3]O$ was obtained at higher pressures (40(2) GPa), while $Te_4O_7[CO_3]$ was synthesized at moderate pressures (20(2) GPa). The crystal structures of both compounds were determined from synchrotron single crystal X-ray diffraction data and confirmed by density functional theory-based calculations. For $Te[CO_3]O$ the experimental Raman data were accurately reproduced by a Raman spectrum derived from the calculations. Both carbonates belong to the family of sp^2-carbonates and are characterized by the presence of trigonal-planar $[CO_3]^{2-}$-groups. While the crystal structure of $Te[CO_3]O$ is rather simple, $Te_4O_7[CO_3]$ is a layered compound with layers of $[CO_3]^{2-}$-groups alternating with complex Te−O-layers. Our DFT-based calculations show that stereochemically active lone electron pairs are present in both crystal structures at elevated pressures. The successful synthesis of $Te[CO_3]O$ is a significant enlargement of the crystal chemistry of carbonates, as it demonstrates that anhydrous carbonates of chalcogenide group elements hosting no further cations can be synthesized. Excluding the noble gases, the chalcogenide group was the last main group of the periodic table where such carbonates were not known up to now.



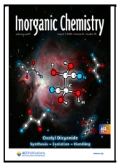
INTRODUCTION

The crystal chemistry of chemically simple anhydrous sp^2-carbonates attracted significant attention in the last years due to a growing number of high-pressure experiments. Such "conventional" carbonates are characterized by trigonal-planar $[CO_3]^{2-}$-groups as their defining structural building blocks in which sp^2-hybrid orbitals are present between the central carbon atom and the surrounding oxygen atoms, and contain only one type of cation.[1,2] Until recently, such carbonates were limited to those containing alkali and alkaline earth cations (e.g., $Na_2[CO_3]$ or $Ca[CO_3]$) or 3*d* transition metal cations (e.g., $Mn[CO_3]$ to $Zn[CO_3]$ and $Cd[CO_3]$).[3−9] A great step forward for understanding the crystal chemistry of carbonates was the synthesis of $Be[CO_3]$, the last missing member of the alkaline earth metal carbonates, at moderate pressures and the discovery that its high-pressure polymorph is isostructural to $Mg[CO_3]$,[10,11] following the "pressure-homologue rule".[12]

The next significant expansion of the crystal chemistry of sp^2-carbonates was the discovery that chemically simple carbonates hosting M^{3+} metal cations such as $Al_2[CO_3]_3$, $Fe_2[CO_3]_3$ or $Cr_2[CO_3]_3$ can be obtained at moderate pressures.[13−15] Moreover, $Al_2[CO_3]_3$ was the first representative of a carbonate containing an element from the boron group. The same experimental approach also allowed the synthesis of the anhydrous carbonates $U[CO_3]_2$ and $Ti_2O_3[CO_3]$ hosting M^{4+} metal cations.[16,17] The very recent description of the first carbonate of silicon, $Si[CO_3]_2$, demonstrated unambiguously that not only metals but also metalloid cations can form chemically simple carbonates.[18] The latest enlargement of the carbonate chemistry was the synthesis of $(IO_2)_2[CO_3]$.[19] This di-iodyl carbonate hosts nonmetal I^{5+} cations and it was the first compound containing only a halogen group element as a cation in a carbonate. This discovery was specifically of interest after the synthesis of the mixed-anion iodide carbonate $Na_5(CO_3)_2I$, where iodine is not present as a cation but I^- anions are present next to $[CO_3]^{2-}$-groups.[20]

In contrast to carbonates with cations from groups 1−15 and 17, no chemically simple carbonate or oxide-carbonates of a chalcogenide has been characterized up to now. Therefore, a timely and relevant question is whether a chalcogen can be

Received: May 24, 2026
Revised: July 8, 2026
Accepted: July 9, 2026
Published: July 17, 2026



ACS Publications
© 2026 The Authors. Published by American Chemical Society

https://doi.org/10.1021/acs.inorgchem.6c02651
Inorg. Chem. 2026, 65, 17749−17755

Downloaded from pubs.acs.org/inocaj/article-pdf/65/30/17749/6599429/acs.inorgchem.6c02651.pdf by DEUTSCHES ELEKTRONEN-SYNCHROTRON user on 27 August 2026

incorporated into carbonates as the only cation species. Here, we address this question by investigating tellurium as a potential cation. Tellurium is a metalloid and known to occur as a cation (e.g., in $Te^{IV}O_2$ or $Te^{VI}O_3$), as well as an anion (e.g., in Sb_2Te_3, PbTe or $AuTe_2$) with different oxidation states.[21−25] This flexibility makes it a promising candidate to form a compound hosting $[CO_3]^{2-}$-groups. Moreover, in the naturally occurring mineral mroseite ($CaTeO_2[CO_3]$) the tellurium atoms are present as a cation, but next to calcium atoms.[26] In the complex dialkyltelluroxane carbonates $(Me_2TeOTeMe_2[CO_3])_n$ or $HO(CH_2)_4TeOTe(CH_2)_4[CO_3]$-$Te(CH_2)_4OH{\cdot}H_2O$ further H_2O, CH_3 or $(CH_2)_4$ groups are stabilizing the crystal structure.[27] Hence it is unclear, if a chemically simple carbonate of tellurium i. e. of a chalcogenide can be synthesized.

Tellurium compounds are of general interest due to the presence of stereochemically active lone electron pairs. The presence of such lone electron pairs significantly influences the crystal structure and determines their chemical and physical properties to a significant extent. Hence, characterizing such compounds is of great interest for inorganic chemistry.[28−31] For example, it is well established that tellurites hosting Te^{4+} cations have in most cases stereoactive $5s^2$ lone electron pairs and that the nonlinear optical properties of compounds such as TeO_2 are affected by these lone electron pairs.[32−34] We have demonstrated in the past that density functional theory (DFT) based calculations can be employed to visualize the stereochemically active lone electron pairs (e.g., in $Bi_2Ga_4O_9$, in Pb_2SnO_4 and in $Sb_2O_2[CO_3]$) at elevated pressures.[35−37]

In order to understand if an anhydrous carbonate of tellurium can be synthesized in analogy to the halogen carbonate $(IO_2)_2[CO_3]$ or the chemically simple carbonates such as $Be[CO_3]$, $Al_2[CO_3]_3$ or $U[CO_3]_2$ we investigated the reaction between TeO_2 and CO_2 at pressures of 20 GPa and of 40 GPa.[10,11,13,19] In TeO_2 four-valent Te^{4+} cations are present with an ionic radius ($r(Te^{4+})$ = 0.97 Å) similar to those often observed for the cations in "conventional" calcite-type carbonates such as $Ca[CO_3]$ ($r(Ca^{2+})$ = 1.00 Å). The ionic radius of Te^{4+} is nearly identical to those of I^{5+} ($r(I^{5+})$ = 0.95 Å) in $(IO_2)_2[CO_3]$ and slightly larger than of U^{4+} ($r(U^{4+})$ = 0.89 Å) in $U[CO_3]_2$.[6,9,16,19,38]

RESULTS AND DISCUSSION

The high-pressure experiments were carried out in laser-heated diamond anvil cells (LH-DACs). In a first step, a commercially available TeO_2 powder was compacted between a glass plate and a diamond and then placed on the culet of the bottom diamond of the DAC. In a second step, cryogenic loading was employed to condense CO_2−I (dry ice) directly into the sample chamber of the DAC (see SI). The DAC was cooled down to ≈100 K and CO_2 was condensed into the sample chamber of the DAC until the chamber was filled and the TeO_2 power compact was completely covered. In the last step, the DAC was closed tightly and compressed to the target pressure of the experiment without intermediate heating. After the cryogenic loading CO_2−I is present in the sample chamber. During cold compression of the DAC a single phase transition from CO_2−I ($Pa\bar{3}$) to CO_2−III ($Cmca$) occurs in a broad (≈5 GPa) pressure range around ≈12 GPa.[39−41] At 20 GPa as well as at 40 GPa CO_2−III is present before the laser heating. At pressures above ≈12 GPa and ≤40 GPa heating CO_2−III will result in the formation of the high-temperature polymorphs CO_2−II or CO_2−IV, depending on the temperature.[41−43] Above ≈25 GPa also CO_2−V ($I\bar{4}2d$) is present, which is the stable CO_2-polymorph up to very high pressures (>100 GPa).[41,44]

In the first experiment the TeO_2 + CO_2 mixture was compressed to 40(2) GPa without intermediate heating (Figure 1 a) and laser-heated from both sides up to a maximum temperature of ≈1600(200) K (Figure 1b). The heating time was 30 min. After the heating, metastable CO_2−III is still present around the heated area in the sample chamber (Figure 1b). In addition, we could observe the characteristic Raman modes of CO_2−V in the laser heated area (Figure 1d). The experimental Raman spectrum of CO_2−V is in very good agreement with the one derived from our DFT-based calculations (Figure 2a). In addition, we observed some minor Raman peaks of the low-pressure high-temperature CO_2 polymorph II. (Figure 2a). In order to determine if a reaction between TeO_2 and CO_2 had occurred we employed spatially resolved Raman spectroscopy on a grid across the sample chamber. We found that an unknown phase is present in the sample chamber after heating (Figure 1c,e,f), which shows a strong Raman mode at ≈1140 cm^{-1} (Figure 2b). Raman modes occurring at this wavenumber are characteristic for the

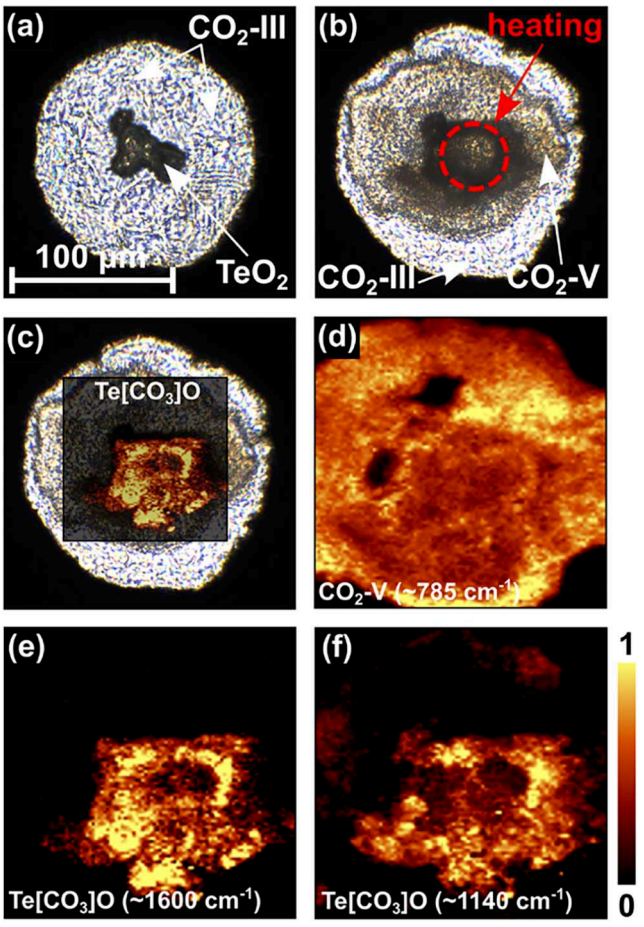


Figure 1. (a) Unheated TeO_2 powder in the sample chamber of the DAC together with CO_2−III at 40(2) GPa. (b) TeO_2 + CO_2 mixture after laser heating to ≈1600(200) K at 40(2) GPa. (c) Raman map of $Te[CO_3]O$ after laser heating overlaid on a picture of the sample chamber. (d) Raman map of CO_2−V (≈785 cm^{-1}). Raman maps of different $Te[CO_3]O$ Raman modes: (e) ≈1600 cm^{-1} and (f) ≈1140 cm^{-1}.

Downloaded from pubs.acs.org/inocaj/article-pdf/65/30/17749/6599298/acs.inorgchem.6c02651.pdf by DEUTSCHES ELEKTRONEN-SYNCHROTRON user on 27 August 2026

https://doi.org/10.1021/acs.inorgchem.6c02651
Inorg. Chem. 2026, 65, 17749−17755

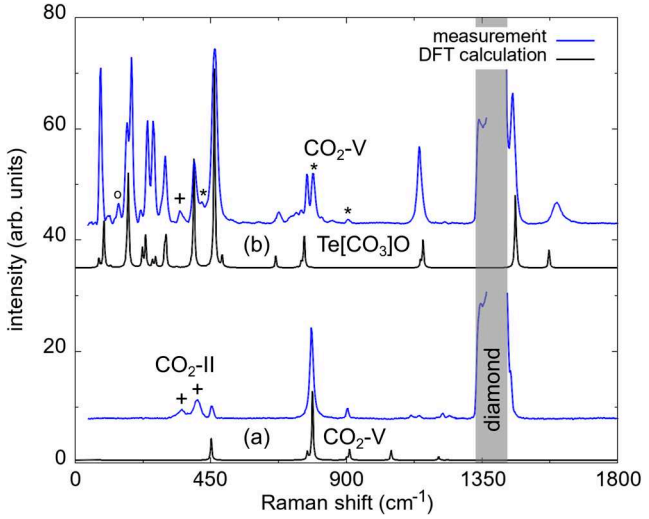


Figure 2. Raman spectroscopy at 40(2) GPa after laser heating the TeO_2 + CO_2 mixture: (a) Raman spectra for CO_2−V. (b) Raman spectra for $Te[CO_3]O$. Experimental Raman spectra are shown in blue, DFT-based calculations are shown in black. The Raman shifts of the theoretical spectra were scaled by 1−3%. Peaks of CO_2−II in the Raman spectrum of CO_2−V are marked by a cross (+). Peaks of CO_2−V in the Raman spectrum of $Te[CO_3]O$ are marked by an asterisk (*) and of CO_2−II by a cross (+). A small Raman peak at ≈200 cm^{-1} could not be assigned to $Te[CO_3]O$ or any CO_2 polymorph. The Raman mode is marked by a circle (°).

C−O stretching mode in a $[CO_3]^{2-}$-group of "conventional" sp^2-carbonates hosting cations with similar ionic radius such as $Mg[CO_3]$ or $Ca[CO_3]$.[45,46] In addition, our Raman maps (Figure 1e,f) reveal that a noticeable Raman mode at ≈1600 cm^{-1} (Figure 2b) belongs to the same phase. A significant Raman signal at such wavenumbers, indicating the presence of a $[CO_3]^{2-}$-group, was also observed in $(IO_2)[CO_3]$.[19] From the distribution of the of the new phase in the Raman map across the heated area we infer that most of the TeO_2 powder reacted with the CO_2 during the formation of the unknown carbonate phase.

In order to determine the crystal structure of the unknown phase we used synchrotron-based X-ray diffraction. First, X-ray powder diffraction data were collected on a 2D grid across the sample chamber. Afterwards we collected diffraction data suitable for single crystal X-ray diffraction on selected grid positions with unidentified reflections. The results from the single crystal structure solution and refinement show that the unknown phase is an anhydrous and chemically simple tellurium oxide-carbonates with $Te[CO_3]O$ composition. $Te[CO_3]O$ crystallizes in the monoclinic space group $P2_1/c$ with Z = 4 (Figure 3a). The lattice parameters at 40(2) GPa are a = 4.3690(3) Å, b = 5.606(2) Å, c = 8.4270(8) Å and β = 90.32(1)° (V = 206.41(7) $Å^3$). The very low R_1-value of 3.0% and the high reflection-to-parameter-ratio (10.5:1) are indicative of a very good structure refinement. In addition, the displacement parameters of the light carbon and oxygen atoms could be refined anisotropically next to the heavy tellurium atoms, confirming the very high quality of the collected diffraction data. No constraints or restraints had to be introduced for the structure refinement. The experimental structural model is in very good agreement with the one derived from our DFT-based full geometry optimization (Table S1). Moreover, the experimental Raman spectrum is

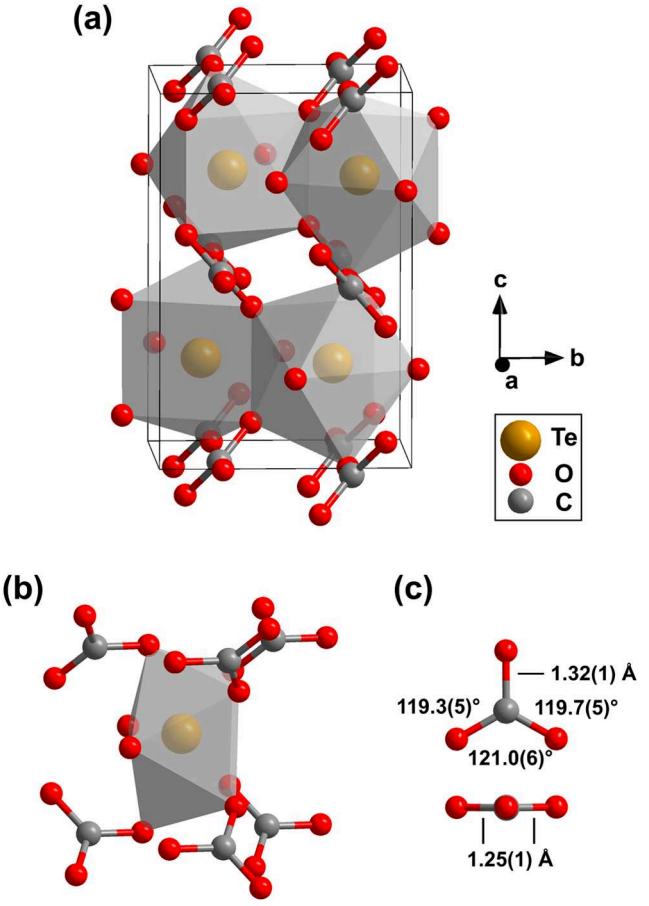


Figure 3. (a) Crystal structure of $Te[CO_3]O$ obtained from synchrotron single-crystal X-ray diffraction at 40(2) GPa ($P2_1/c$, Z = 4). (b) Coordination polyhedron of the tellurium atom by oxygen. (c) Geometry of the $[CO_3]^{2-}$-group from single-crystal X-ray diffraction.

accurately reproduced by a theoretical Raman spectrum obtained from our DFPT-calculations (Figure 2b), confirming that the structural model is appropriate ($P2_1/c$). There are 36 Raman active modes. However, we noticed, that the β-angle is very close to 90° (SC-XRD: 90.32(1)°), hence we tested the experimental structural model using the PLATON/checkCIF program in order to check for a higher space group symmetry.[47] PLATON/checkCIF suggests the orthorhombic space group *Pbcm* as a possible higher symmetry. Performing a reasonably successful structure solution and refinement in space group *Pbcm* was not possible. Due to symmetry constraints on the tellurium atom position the R_1-value is very high for a refinement in the orthorhombic space group (≥20%). Hence, we think that the monoclinic ($P2_1/c$) structural model for $Te[CO_3]O$ is appropriate for our experimental data.

$Te[CO_3]O$ is a chemically simple oxide-carbonate. It belongs to the family of anhydrous sp^2-carbonates hosting $[CO_3]^{2-}$-groups as central building blocks (Figure 3). The $[CO_3]^{2-}$-groups are nearly ideally trigonal-planar with C−O bond distances of 1.25(1) Å and 1.32(1) Å (Figure 3c). The experimental O−C−O angles are all very similar 119.3(5)°, 119.7(5)° and 121.0(6)°. The C−O bond distances (1.25 Å and 1.30 Å) and O−C−O angles (119.4° and 120.3°) derived from our DFT-based calculations reproduce the experimental values with the expected uncertainties. The Mulliken

Downloaded from pubs.acs.org/inocaj/article-pdf/65/30/17749/6599298/acs.inorgchem.6c02651.pdf by DEUTSCHES ELEKTRONEN-SYNCHROTRON user on 27 August 2026

https://doi.org/10.1021/acs.inorgchem.6c02651
Inorg. Chem. 2026, 65, 17749−17755

population analysis yielded nearly identical values for the C−O bonds (0.94 $e^-/Å^3$ and 0.79 $e^-/Å^3$) and suggests a strong covalent bonding within the $[CO_3]^{2-}$-group. The remaining oxygen atom, which is not part of the $[CO_3]^{2-}$-group, is only connected to two tellurium atoms. The experimental (1.93(1) Å) and calculated (2.00 Å) Te−O bond distances match well. Each tellurium atom is coordinated by 8 oxygen atoms (Figure 3b). Two of these oxygens are not part of a $[CO_3]^{2-}$-group. In contrast to the complex dialkyltelluroxane carbonates $(Me_2TeOTeMe_2[CO_3])_n$ or $HO(CH_2)_4TeOTe(CH_2)_4[CO_3]$-$Te(CH_2)_4OH{\cdot}H_2O$ no further H_2O, CH_3 or $(CH_2)_4$ groups are required to stabilize the crystal structure of $Te[CO_3]O$.[27] The geometry of the $[CO_3]^{2-}$-groups in the complex dialkyltelluroxane carbonates or in mroseite are in agreement with the geometry derived for the $[CO_3]^{2-}$-group in $Te[CO_3]O$ at elevated pressures hosting no further cations or building blocks.[26,27]

In a second experiment the TeO_2−CO_2 system was investigated at lower pressures (20(2) GPa), in order to understand if $Te[CO_3]O$ can also be obtained at significantly lower pressures. From our single crystal X-ray diffraction data collected at 20(2) GPa we found that $Te[CO_3]O$ could not be synthesized at this pressure. However, our data clearly show that a reaction between TeO_2 and CO_2 had occurred. We solved the crystal structure of the second tellurium carbonate, which was present across the heated area in the sample chamber of the DAC. The second anhydrous carbonate phase at 20(2) GPa has $Te_4O_7[CO_3]$ composition. The oxide-carbonate $Te_4O_7[CO_3]$ crystallizes in the acentric orthorhombic space group *Iba*2 with Z = 8 (Figure 4a). The lattice parameters are a = 21.576(1) Å, b = 10.671(2) Å and c = 5.5405(2) Å (V = 1275.6(2) $Å^3$). The crystal structure refinement is robust (R_1-value = 3.3% and reflection-to-parameter-ratio = 15.8:1). The displacement parameters of all 16 symmetrically independent atoms could be refined anisotropically without introducing any constraints or restraints, confirming the very high quality of the collected diffraction data. In addition, our DFT-based full geometry optimization confirmed the experimental structural model (Table S2). Our XRD data show the presence of remaining acentric TeO_2-$P2_12_12_1$, preventing an unambiguous detection of the second harmonic generation (SHG) signal of $Te_4O_7[CO_3]$-*Iba*2.

$Te_4O_7[CO_3]$ belongs also to the family of anhydrous sp^2-carbonates, in particular to the subgroup of oxide-carbonates. It has a complex layered crystal structure (Figure 4a). One layer consists of trigonal-planar $[CO_3]^{2-}$-groups (Figure 4b). Similar to $Te[CO_3]O$ the $[CO_3]^{2-}$-groups in $Te_4O_7[CO_3]$ are nearly ideal trigonal-planar with C−O bond distances between 1.27(1) Å and 1.28(1) Å and O−C−O angles between 117.1(8)° and 122.0(7)°. The C−O bond distances (1.25 Å to 1.23 Å) and O−C−O angles are in good agreement with our DFT-calculations. Our Mulliken population analysis reveals strong covalent C−O bonds (0.95 $e^-/Å^3$ to 0.79 $e^-/Å^3$) within the $[CO_3]^{2-}$-groups. The Mulliken populations are in agreement with the populations derived for $Te[CO_3]O$ at 40 GPa. The second layer of the $Te_4O_7[CO_3]$ crystal structure consists of a complex network of tellurium and oxygen atoms with "Te_4O_7"-composition. All remaining oxygen atoms, which are not part of the $[CO_3]^{2-}$-groups, are involved. The Mulliken population analysis of the Te−O bonds within the layer yields significantly lower values (between 0.16 $e^-/Å^3$ and 0.30 $e^-/Å^3$) than for the C−O bonds. The interactions between the

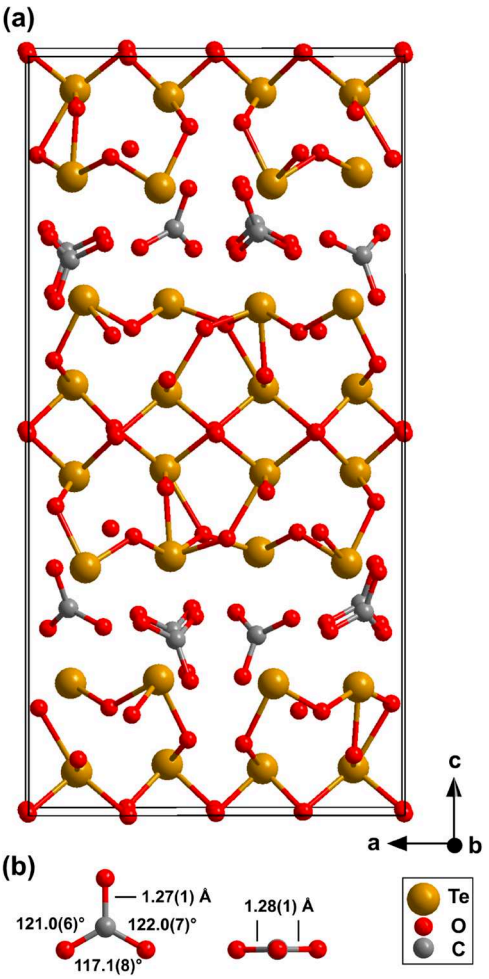


Figure 4. (a) Crystal structure of $Te_4O_7[CO_3]$ obtained from synchrotron single-crystal X-ray diffraction at 20(2) GPa (*Iba*2, Z = 8). (b) Geometry of the $[CO_3]^{2-}$-group from single-crystal X-ray diffraction.

tellurium atoms within the layer and the oxygen atoms of the $[CO_3]^{2-}$-groups are even weaker (≤0.10 $e^-/Å^3$). It is worthwhile to note that in the TeO_2−SO_3 system compounds such as $TeO[SO_4]$, $Te_2O_3[SO_4]$ and $Te_4O_3[SO_4]_5$ with a similar tellurium−oxygen sublattice have been found.[22,48] Hence, it is likely that also in the TeO_2−CO_2 system further novel carbonates with different tellurium−oxygen sublattices can be synthesized.

We employed our DFT-based calculations to investigate the electron density distribution in the crystal structure of $Te[CO_3]O$. The calculations clearly show lone electron pairs as umbrella shaped maxima in the electron difference density map, ≈0.7 Å away from the tellurium atom (Figure 5a). The lone electron pairs are stereochemically active. Such stereochemically active lone electron pairs have earlier been observed e. g. in $Bi_2Ga_4O_9$, in Pb_2SnO_4 and in $Sb_2O_2[CO_3]$ at elevated pressures.[35−37] The existence of the lone electron pairs of the tellurium atom results in an asymmetric shape of the Te−O coordination polyhedron in $Te[CO_3]O$ (Figure 3b). We performed the same analysis for the crystal structure of $Te_4O_7[CO_3]$. Similar to $Te[CO_3]O$ our DFT calculations clearly show lone electron pairs as umbrella shaped maxima in the electron difference density map (Figure 5b). Both compounds are insulators. The DFT-GGA-PBE calculations

Downloaded from pubs.acs.org/inocaj/article-pdf/65/30/17749/6599298/acs.inorgchem.6c02651.pdf by DEUTSCHES ELEKTRONEN-SYNCHROTRON user on 27 August 2026

https://doi.org/10.1021/acs.inorgchem.6c02651
Inorg. Chem. 2026, 65, 17749−17755

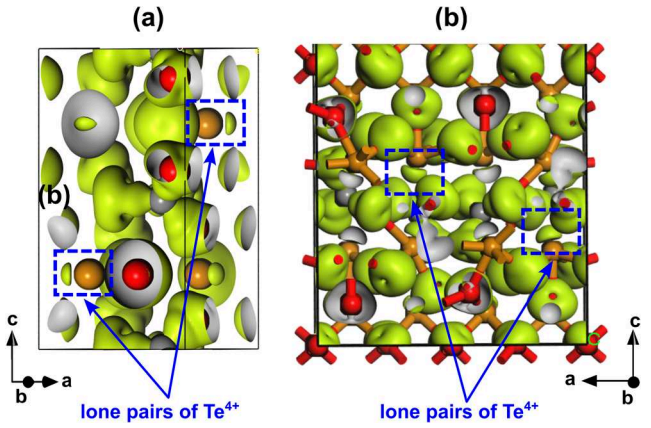


Figure 5. Electron difference density map (a) of $Te[CO_3]O$ and (b) of $Te_4O_7[CO_3]$ from DFT-based calculations. The stereochemically active lone electron pairs in both crystal structures manifest themselves as umbrella shaped maxima in the map, about 0.7 Å away from the Te^{4+} cation. The isosurface shown represents electron difference densities of 0.04 $e^-/Å^3$.

yield weakly pressure-dependent band gaps of ≈2.3 eV for $Te_4O_7[CO_3]$ and ≈2.7 eV for $Te[CO_3]O$, but it is well established that these values will be significantly underestimated.

After we established that our DFT-calculations accurately reproduce the experimentally determined structures of $Te[CO_3]O$ as well as of $Te_4O_7[CO_3]$ at their synthesis pressures, we employed further calculations to derive the *p*,*V*-relation for both phases. From the calculations we predict that $Te[CO_3]O$ is undergoing an isostructural phase transition during decompression. The calculated *p*,*V*-data of the different $Te[CO_3]O$ phases were fitted separately with an equation of state (EoS) in order to determine the bulk modulus K_0 and its pressure derivative K_p (Figure S3). We obtained a bulk modulus of K_0 = 80.0(6) GPa with K_p = 5.76(4) for the high-pressure phase of $Te[CO_3]O$ and a significantly lower bulk modulus of K_0 = 32.4(6) GPa with K_p = 6.2(1) for its low-pressure phase. The ambient pressure bulk modulus of the high-pressure phase is in the same range than reported for other "conventional" carbonates hosting medium sized cations, such as $Ca[CO_3]$ (67(2) GPa) or $Mg[CO_3]$ (107(1) GPa).[49] For $Te_4O_7[CO_3]$ we derived a bulk modulus of K_0 = 51(4) GPa with K_p = 6.7(4) (Figure S4). This value is in between the bulk modulus derived for the low- and high-pressure phase of $Te[CO_3]O$. The pressure-dependent compressibility K_p is relatively large in comparison with other "conventional" carbonates. However, the values are similar to the ones derived for $(IO_2)_2[CO_3]$ at similar pressures.[19]

CONCLUSION

In summary we have synthesized two anhydrous carbonates of tellurium at elevated pressures, $Te[CO_3]O$ (40(2) GPa), and $Te_4O_7[CO_3]$ (20(2) GPa), by a reaction of TeO_2 with CO_2. Both belong to the subgroup of oxide-carbonates. Single crystal X-ray diffraction was employed to determine the crystal structure of both phases after their synthesis inside the LH-DAC. DFT-based calculations were used to confirm the experimental structural models of both compounds. The crystal structures of both phases are characterized by trigonal-planar $[CO_3]^{2-}$-groups and hence $Te[CO_3]O$ and $Te_4O_7[CO_3]$ belong to the family of anhydrous sp^2-carbonates. Moreover, in both phases four-valent Te^{4+}-cations are present. The stereochemically active lone electron pairs manifest themselves as umbrella shaped maxima in the electron difference density map, about 0.7 Å away from the tellurium atoms in both phases in our DFT-calculations. The successful synthesis of $Te[CO_3]O$ answers the question if an anhydrous carbonate of a chalcogenide group element, hosting no further cations, can be synthesized. This is a significant extension of the crystal chemistry of carbonates as, neglecting the noble gases, the chalcogenide group was the last main group of the periodic table where such an anhydrous carbonate was not known up to now. In addition, after the recent synthesis of $Si[CO_3]_2$,[18] the synthesis of $Te[CO_3]O$ confirms that metalloid cations can form chemically simple carbonates or oxide-carbonates. Moreover, we are confident that the synthesis of $Te[CO_3]O$ as well as of $Te_4O_7[CO_3]$ provides a roadmap for the synthesis of further novel carbonates hosting metalloid or nonmetal cations e. g. of chalcogen group elements such as selenium or sulfur. This would provide a broader basis for a systematic crystal chemistry of anhydrous metalloid or nonmetal carbonates. In addition, it would facilitate the investigation of compounds characterized by the presence of lone electron pairs at elevated pressures, which in turn may have interesting chemical and physical properties.[28−34,50]

METHODS

Commercial tellurium dioxide (TeO_2) powder was used as starting material for the high-pressure experiments (99.995% purity, Merck KGaA, Darmstadt, Germany). The high-pressure experiments were carried out in Boehler-Almax type diamond anvil cells (DACs).[51] CO_2 (Nippon gases, purity ≥99.996%) was loaded cryogenically into into the DAC as dry ice by a custom-built cryogenic loading system.[19] The TeO_2 powder was laser-heating from both sides using a custom-built setup equipped with a Coherent Diamond K-250 pulsed CO_2 laser (λ = 10600 nm) at the target pressures of the different experiments.[46] For high-pressure Raman spectroscopy, we employed an Oxford Instruments WITec α 300R Raman imaging microscope equipped with an Olympus SLMPan N 50× objective. The measurements were performed using the 532 nm laser and the 1200 grooves mm^{-1} grating of the WITec UHTS 300S (VIS-NIR) spectrograph. High-pressure single-crystal synchrotron X-ray diffraction experiments were carried out at PETRA III (DESY) in Hamburg, Germany, at the extreme conditions beamline P02.2 and at the ESRF in Grenoble, France, at the Materials Science Beamline line ID11.[52,53] First-principles calculations were carried out within the framework of density functional theory (DFT), employing the Perdew−Burke−Ernzerhof (PBE) exchange-correlation functional and the plane wave/pseudopotential approach implemented in the CASTEP simulation package.[54−56] In addition, we employed a correction scheme for van der Waals (v.d.W.) interactions.[57] A detailed description of the experimental and computational methods is available in the Supporting Information.

ASSOCIATED CONTENT

Supporting Information

The Supporting Information is available free of charge at https://pubs.acs.org/doi/10.1021/acs.inorgchem.6c02651.

Experimental and computational details of the experiments and the results of the single-crystal structure solution and DFT-based calculations (PDF)

Accession Codes

Deposition Numbers 2531481−2531482 contain the supplementary crystallographic data for this paper. These data can be

Downloaded from pubs.acs.org/inocaj/article-pdf/65/30/17749/6599298/acs.inorgchem.6c02651.pdf by DEUTSCHES ELEKTRONEN-SYNCHROTRON user on 27 August 2026

https://doi.org/10.1021/acs.inorgchem.6c02651
Inorg. Chem. 2026, 65, 17749−17755

obtained free of charge via the joint Cambridge Crystallographic Data Centre (CCDC) and Fachinformationszentrum Karlsruhe Access Structures service.

AUTHOR INFORMATION

Corresponding Author

Dominik Spahr − *Goethe University Frankfurt, Institute of Geosciences, 60438 Frankfurt, Germany; Stony Brook University, Department of Geosciences, Stony Brook, New York 11794-2100, United States;* orcid.org/0000-0003-0489-5270; Email: d.spahr@kristall.uni-frankfurt.de

Authors

Lkhamsuren Bayarjargal − *Goethe University Frankfurt, Institute of Geosciences, 60438 Frankfurt, Germany;* orcid.org/0000-0002-5513-591X

Ninel Sharapova − *Goethe University Frankfurt, Institute of Geosciences, 60438 Frankfurt, Germany*

Valentin Kovalev − *Goethe University Frankfurt, Institute of Geosciences, 60438 Frankfurt, Germany*

Andrey Aslandukov − *Goethe University Frankfurt, Institute of Inorganic and Analytical Chemistry, 60438 Frankfurt, Germany;* orcid.org/0000-0003-0988-6066

Fariia I. Akbar − *Goethe University Frankfurt, Institute of Inorganic and Analytical Chemistry, 60438 Frankfurt, Germany;* orcid.org/0000-0002-6016-5849

Elena Bykova − *Goethe University Frankfurt, Institute of Geosciences, 60438 Frankfurt, Germany;* orcid.org/0000-0001-8652-024X

Maxim Bykov − *Goethe University Frankfurt, Institute of Inorganic and Analytical Chemistry, 60438 Frankfurt, Germany;* orcid.org/0000-0003-0248-1728

Victor Milman − *Dassault Systèmes BIOVIA, Cambridge CB4 0FJ, United Kingdom;* orcid.org/0000-0003-2258-1347

Nico Giordano − *Deutsches Elektronen-Synchrotron DESY, 22607 Hamburg, Germany;* orcid.org/0000-0001-9518-1251

Björn Winkler − *Goethe University Frankfurt, Institute of Geosciences, 60438 Frankfurt, Germany;* orcid.org/0000-0001-8029-478X

Complete contact information is available at: https://pubs.acs.org/10.1021/acs.inorgchem.6c02651

Notes

The authors declare no competing financial interest.

ACKNOWLEDGMENTS

We gratefully acknowledge funding from the DFG (WI1232 and BA4020). D.S. gratefully acknowledges financial support by the Fulbright Program. E.B. and M.B. acknowledge the support of the DFG Emmy-Noether Program (projects BY101/2-1 and BY112/2-1) and the support by the Johanna-Quandt-Stiftung. M.B. acknowledge the support by the LOEWE program. B.W. is grateful for support by the Dassault Systèmes Science Ambassador program. We acknowledge DESY (Hamburg, Germany), a member of the Helmholtz Association HGF, for the provision of experimental facilities. Parts of this research were carried out at PETRA III, beamline P02.2. We acknowledge the European Synchrotron Radiation Facility (ESRF) for provision of synchrotron radiation facilities under proposal number CH-7327 and we would like to thank Jon Wright for assistance and support in using beamline ID11 (doi: 10.15151/ESRF-ES-2160870041).

REFERENCES

(1) Winkler, B.; Zemann, J.; Milman, V. Aplanarity of CO_3 groups: A theoretical investigation. *Acta. Cryst. B* **2000**, *56*, 648−653.

(2) *Carbonates: Mineralogy and Chemistry*; Reeder, R. J., Ed.; De Gruyter: Berlin, Boston, 1983.

(3) Graf, D. L. Crystallographic tables for the rhombohedral carbonates. *Am. Mineral.* **1961**, *46*, 1283−1316.

(4) Seidel, H.; Viswanathan, K.; Johannes, W.; Ehrhardt, H. Darstellung, Struktur und Eigenschaften von Kupfer(II)-Carbonat. *Z. Anorg. Allg. Chem.* **1974**, *410*, 138−148.

(5) Ehrhardt, H.; Seidel, H.; Schweer, H. Hochdrucksynthesen einiger Carbonate mit überkritischem CO_2. *Z. Anorg. Allg. Chem.* **1980**, *462*, 185−198.

(6) Effenberger, H.; Mereiter, K.; Zemann, J. Crystal structure refinements of magnesite, calcite, rhodochrosite, siderite, smithonite, and dolomite, with discussion of some aspects of the stereochemistry of calcite type carbonates. *Z. Kristallogr.* **1981**, *156*, 233−243.

(7) Liu, L.-G.; Lin, C.-C. A calcite → aragonite-type phase transition in $CdCO_3$. *Am. Mineral.* **1997**, *82*, 643−646.

(8) Dusek, M.; Chapuis, G.; Meyer, M.; Petricek, V. Sodium carbonate revisited. *Acta Crystallogr., Sect. B:Struct. Sci.* **2003**, *59*, 337−352.

(9) Antao, S. M.; Hassan, I. The orthorhombic structure of $CaCO_3$, $SrCO_3$, $PbCO_3$ and $BaCO_3$: Linear structural trends. *Can. Mineral.* **2009**, *47*, 1245−1255.

(10) Spahr, D.; Bayarjargal, L.; Bykova, E.; Bykov, M.; Reuter, T. H.; Brüning, L.; Jurzick, P. L.; Wedek, L.; Milman, V.; Wehinger, B.; Winkler, B. Synthesis and crystal structure of acentric anhydrous beryllium carbonate $Be[CO_3]$. *Chem. Commun.* **2024**, *60*, 10208−10211.

(11) Spahr, D.; Bayarjargal, L.; Bykova, E.; Bykov, M.; Brüning, L.; Kovalev, V.; Milman, V.; Wright, J.; Winkler, B. 6-Fold-Coordinated Beryllium in Calcite-Type Be $Be[CO_3]$. *Inorg. Chem.* **2024**, *63*, 19513−19517.

(12) Neuhaus, A. Synthese Strukturverhalten und Valenzzustände der anorganischen Materie im Bereich hoher und höchster Drücke. *Chimia* **1964**, *18*, 93−103.

(13) Bayarjargal, L.; Spahr, D.; Milman, V.; Marquardt, J.; Giordano, N.; Winkler, B. Anhydrous aluminium carbonates and isostructural compounds. *Inorg. Chem.* **2023**, *62*, 13910−13918.

(14) Bayarjargal, L.; Spahr, D.; Bykova, E.; Wang, Y.; Giordano, N.; Milman, V.; Winkler, B. High-Pressure Synthesis of an Iron Carbonate, $Fe_2[CO_3]_3$. *Inorg. Chem.* **2024**, *63*, 21637−21644.

(15) Wang, Y.; Bayarjargal, L.; Bykov, M.; Bykova, E.; Spahr, D.; Glazyrin, K.; Milman, V.; Winkler, B. Cr^{3+}-Containing Carbonates and Cr_2O_3-Pbcn at Extreme Conditions. *Inorg. Chem.* **2025**, *64*, 4996−5003.

(16) Spahr, D.; Bayarjargal, L.; Bykova, E.; Bykov, M.; Murphy, G. L.; Kegler, P.; Milman, V.; Giordano, N.; Winkler, B. High-pressure synthesis of $U_2[CO_3]_3$ and $U[CO_3]_2$ as potential host phases for uranium in the Earth's mantle. *Commun. Chem.* **2026**, *9*, 112.

(17) Bayarjargal, L.; Spahr, D.; Milman, V.; Giordano, N.; Glazyrin, K.; Winkler, B. Synthesis and Characterization of Ti4+ Containing Carbonates $Ti[CO_4]$ and $Ti_2O_3[CO_3]$. *Inorg. Chem.* **2025**, *64*, 21893−21902.

(18) Spahr, D.; Bayarjargal, L.; Kovalev, V.; Sharapova, N.; Brüning, L.; Jurzick, P. L.; Sebastian, S. S.; Bykov, M.; Milman, V.; Glazyrin, K.; Bykova, E.; Winkler, B. Silicon carbonate,$Si[CO_3]_2$, is a potential carbon host in the deep Earth. *Sci. Adv.* **2026**, *12*, No. eaee5766.

(19) Spahr, D.; Bayarjargal, L.; Brüning, L.; Kovalev, V.; Bykova, E.; Bykov, M.; Milman, V.; Mezouar, M.; Winkler, B. Synthesis and Crystal Structure of Anhydrous Di-iodyl Carbonate $(IO_2)_2[CO_3]$, Hosting I^{5+}-Cations. *JACS Au* **2025**, *5*, 4675−4680.

(20) Yin, Y.; Dubrovinsky, L.; Aslandukov, A.; Aslandukova, A.; Akbar, F. I.; Zhou, W.; Hanfland, M.; Abrikosov, I.; Dubrovinskaia, N.

Downloaded from pubs.acs.org/inocaj/article-pdf/65/30/17749/6599298/acs.inorgchem.6c02651.pdf by DEUTSCHES ELEKTRONEN-SYNCHROTRON user on 27 August 2026

High-Pressure Synthesis of the Iodide Carbonate$Na_5(CO_3)_2I$. *Solids* **2024**, *5*, 333−340.
(21) Worlton, T. G.; Beyerlein, R. A. Structure and order parameters in the pressure-induced continuous transition in TeO_2. *Phys. Rev. B* **1975**, *12*, No. 1899.
(22) Ahmed, M. A. K.; Fjellvåg, H.; Kjekshus, A. Synthesis, structure and thermal stability of tellurium oxides and oxide sulfate formed from reactions in refluxing sulfuric acid. *J. Chem. Soc., Dalton Trans.* **2000**, *29*, 4542−4549.
(23) Das, D.; Malik, K.; Deb, A. K.; Dhara, S.; Bandyopadhyay, S.; Banerjee, A. Defect induced structural and thermoelectric properties of Sb_2Te_3 alloy. *J. Appl. Phys.* **2015**, *118*, No. 045102.
(24) Rousse, G.; Klotz, Sa.; Saitta, A. M.; Rodriguez-Carvajal, J.; McMahon, M. I.; Couzinet, B.; Mezouar, M. Structure of the intermediate phase of PbTe at high pressure. *Phys. Rev. B* **2005**, *71*, No. 224116.
(25) Reithmayer, K.; Steurer, W.; Schulz, H.; de Boer, J. L. High-pressure single-crystal structure study on calaverite, $AuTe_2$. *Acta Crystallogr., Sect. B:Struct. Sci.* **1993**, *49*, 6−11.
(26) Fischer, R.; Pertlik, F.; Zemann, J. The crystal structure of mroseite, $CaTeO_2(CO_3)$. *Can. Mineral.* **1975**, *13*, 383−387.
(27) Beckmann, J.; Bolsinger, J.; Duthie, A. Carbon Dioxide Fixation with Dialkyltellurium(IV) Dihydroxides. *Z. Anorg. Allg. Chem.* **2010**, *636*, 765−769.
(28) Brown, I. D. View of Lone Electron Pairs and Their Role in Structural Chemistry. *J. Phys. Chem. A* **2011**, *115*, 12638−12645.
(29) Luo, M.; Liang, F.; Song, Y.; Zhao, D.; Ye, N.; Lin, Z. Rational Design of the First Lead/Tin Fluorooxoborates $MB_2O_3F_2$ (M = Pb, Sn), Containing Flexible Two-Dimensional $[B_6O_{12}F_6]_\infty$ Single Layers with Widely Divergent Second Harmonic Generation Effects. *J. Am. Chem. Soc.* **2018**, *140*, 6814−6817.
(30) Ok, K. M. Functional layered materials with heavy metal lone pair cations, Pb^{2+}, Bi^{3+}, and Te^{4+}. *Chem. Commun.* **2019**, *55*, 12737−12748.
(31) Laurita, G.; Seshadri, R. Chemistry, Structure, and Function of Lone Pairs in Extended Solids. *Acc. Chem. Res.* **2022**, *55*, 1004−1014.
(32) Hamani, D.; Masson, O.; Thomas, P. Localization and steric effect of the lone electron pair of the tellurium Te^{4+} cation and other cations of the p-block elements. A systematic study. *J. Appl. Crystallogr.* **2020**, *53*, 1243−1251.
(33) Suehara, S.; Thomas, P.; Mirgorodsky, A. P.; Merle-Méjean, T.; Champarnaud-Mesjard, J. C.; Aizawa, T.; Hishita, S.; Todoroki, S.; Konishi, T.; Inoue, S. Localized hyperpolarizability approach to the origin of nonlinear optical properties in TeO_2-based materials. *Phys. Rev. B* **2004**, *70*, No. 205121.
(34) Roginskii, E. M.; Kuznetsov, V. G.; Smirnov, M. B.; Noguera, O.; Duclère, J.-R.; Colas, M.; Masson, O.; Thomas, P. Comparative Analysis of the Electronic Structure and Nonlinear Optical Susceptibility of α-TeO_2 and β-TeO_3 Crystals. *J. Phys. Chem. C* **2017**, *121*, 12365−12374.
(35) Friedrich, A.; Juarez-Arellano, E. A.; Haussühl, E.; Boehler, R.; Winkler, B.; Wiehl, L.; Morgenroth, W.; Burianek, M.; Mühlberg, M. Persistence of the stereochemical activity of the Bi^{3+} lone electron pair in $Bi_2Ga_4O_9$ up to 50 GPa and crystal structure of the high-pressure phase. *Acta Crystallogr., Sect. B:Struct. Sci.* **2010**, *66*, 323−337.
(36) Spahr, D.; Stękiel, M.; Zimmer, D.; Bayarjargal, L.; Bunk, K.; Morgenroth, W.; Milman, V.; Refson, K.; Jochym, D.; Byrne, P. J. P.; Winkler, B. Pressure-induced Pb-Pb bonding and phase transition in Pb_2SnO_4. *Acta Crystallogr., Sect. B:Struct. Sci., Cryst. Eng. Mater.* **2020**, *76*, 979−991.
(37) Spahr, D.; Bayarjargal, L.; Brüning, L.; Bykova, E.; Bykov, M.; Milman, V.; Giordano, N.; Winkler, B. Synthesis and Crystal Structure of $Sb_2O_2[CO_3]$ with Stereochemically Active Lone Electron Pairs at Elevated Pressures. *Z. Anorg. Allg. Chem.* **2026**, No. e70171.
(38) Shannon, R. D. Revised effective ionic radii and systematic studies of interatomic distances in halides and chalcogenides. *Acta Crystallogr., Sect. A* **1976**, *32*, 751−767.
(39) Aoki, K.; Yamawaki, H.; Sakashita, M.; Gotoh, Y.; Takemura, K. Crystal Structure of the High-Pressure Phase of Solid CO_2. *Science* **1994**, *263*, 356−358.
(40) Olijnyk, H.; Jephcoat, A. P. Vibrational studies on CO_2 up to 40 GPa by Raman spectroscopy at room temperature. *Phys. Rev. B* **1998**, *57*, 879−888.
(41) Scelta, D.; Dziubek, K. F.; Ende, M.; Miletich, R.; Mezouar, M.; Garbarino, G.; Bini, R. Extending the Stability Field of Polymeric Carbon Dioxide Phase V beyond the Earth's Geotherm. *Phys. Rev. Lett.* **2021**, *126*, No. 065701.
(42) Yoo, C. S.; Kohlmann, H.; Cynn, H.; Nicol, M. F.; Iota, V.; LeBihan, T. Crystal structure of pseudo-six-fold carbon dioxide phase II at high pressures and temperatures. *Phys. Rev. B* **2002**, *65*, No. 104103.
(43) Datchi, F.; Mallick, B.; Salamat, A.; Ninet, S. Structure of Carbon Dioxide Phase IV: Breakdown of the Intermediate Bonding State Scenario. *Phys. Rev. Lett.* **2012**, *108*, No. 125701.
(44) Datchi, F.; Mallick, B.; Salamat, A.; Ninet, S. Structure of Polymeric Carbon Dioxide CO_2-V. *Phys. Rev. Lett.* **2012**, *108*, No. 125701.
(45) Binck, J.; Bayarjargal, L.; Lobanov, S. S.; Morgenroth, W.; Luchitskaia, R.; Pickard, C. J.; Milman, V.; Refson, K.; Jochym, D. B.; Byrne, P.; Winkler, B. Phase stabilities of $MgCO_3$ and $MgCO_3$-II studied by Raman spectroscopy, X-ray diffraction, and density functional theory calculations. *Phys. Rev. Mater.* **2020**, *4*, No. 055001.
(46) Bayarjargal, L.; Fruhner, C.-J.; Schrodt, N.; Winkler, B. $CaCO_3$ phase diagram studied with Raman spectroscopy at pressures up to 50 GPa and high temperatures and DFT modeling. *Phys. Earth Planet. Inter.* **2018**, *281*, 31−45.
(47) Spek, A. L. Single-crystal structure validation with the program PLATON. *J. Appl. Crystallogr.* **2003**, *36*, 7−13.
(48) Logemann, C.; Bruns, J.; Schindler, L. V.; Zimmermann, V.; Wickleder, M. S. Tellurium Sulfates from Reactions in Oleum and Sulfur Trioxide: Syntheses and Crystal Structures of $TeO(SO_4)$, $Te_4O_3(SO_4)_5$, and $Te(S_2O_7)_2$. *Z. Anorg. Allg. Chem.* **2015**, *641*, 831−837.
(49) Zhang, J.; Reeder, R. J. Comparative compressibilities of calcite-structure carbonates: Deviations from empirical relations. *Am. Mineral.* **1999**, *84*, 861−870.
(50) Lu, W.; Liu, S.; Cai, J.; Ning, P.; Ma, C.; Liu, G.; Wang, H.; Guo, Q.; Zhou, Y.; Wang, M.; Ma, Y. High-pressure and high-temperature modulation of one-dimensional infinite chain in SeO_2. *Appl. Phys. Lett.* **2024**, *124*, No. 142105.
(51) Boehler, R. New diamond cell for single-crystal X-ray diffraction. *Rev. Sci. Instrum.* **2006**, *77*, No. 115103.
(52) Liermann, H.-P.; Konôpková, Z.; Morgenroth, W.; et al. The Extreme Conditions Beamline P02.2 and the Extreme Conditions Science Infrastructure at PETRAIII. *J. Synchrotron Radiat.* **2015**, *22*, 908−924.
(53) Wright, J.; Giacobbe, C.; Majku, M. New opportunities at the Materials Science Beamline at ESRF to exploit high energy nano-focus X-ray beams. *Curr. Opin. Solid State Mater. Sci.* **2020**, *24*, No. 100818.
(54) Hohenberg, P.; Kohn, W. Inhomogeneous Electron Gas. *Phys. Rev.* **1964**, *136*, B864−B871.
(55) Perdew, J. P.; Burke, K.; Ernzerhof, M. Generalized Gradient Approximation Made Simple. *Phys. Rev. Lett.* **1996**, *77*, 3865−3868.
(56) Clark, S. J.; Segall, M. D.; Pickard, C. J.; Hasnip, P. J.; Probert, M. I. J.; Refson, K.; Payne, M. C. First principles methods using CASTEP. *Z. Kristallogr.* **2005**, *220*, 567−570.
(57) Tkatchenko, A.; Scheffler, M. Accurate Molecular Van Der Waals Interactions from Ground-State Electron Density and Free-Atom Reference Data. *Phys. Rev. Lett.* **2009**, *102*, No. 073005.

Downloaded from pubs.acs.org/inocaj/article-pdf/65/30/17749/6599298/acs.inorgchem.6c02651.pdf by DEUTSCHES ELEKTRONEN-SYNCHROTRON user on 27 August 2026

https://doi.org/10.1021/acs.inorgchem.6c02651
Inorg. Chem. 2026, 65, 17749−17755